doi:10.1093/brain/awz026 BRAIN 2019: 142; 1093–1107 | 1093

BRAIN
A JOURNAL OF NEUROLOGY

Functional connectivity associated with tau levels in ageing, Alzheimer's, and small vessel disease

Nicolai Franzmeier,[1] Anna Rubinski,[1] Julia Neitzel,[1] Yeshin Kim,[2,3,4] Alexander Damm,[1] Duk L. Na,[2,4,5] Hee Jin Kim,[2,4] Chul Hyoung Lyoo,[6] Hana Cho,[6] Sofia Finsterwalder,[1] Marco Duering,[1] Sang Won Seo[2,4,7,8] and Michael Ewers[1] for the Alzheimer's Disease Neuroimaging Initiative*

*Data used in preparation of this article were obtained from the Alzheimer's Disease Neuroimaging Initiative (ADNI) database (adni.loni.usc.edu). As such, the investigators within the ADNI contributed to the design and implementation of ADNI and/or provided data but did not participate in analysis or writing of this report. A complete listing of ADNI investigators can be found in the Supplementary material.

In Alzheimer's disease, tau pathology spreads hierarchically from the inferior temporal lobe throughout the cortex, ensuing cognitive decline and dementia. Similarly, circumscribed patterns of pathological tau have been observed in normal ageing and small vessel disease, suggesting a spatially ordered distribution of tau pathology across normal ageing and different diseases. *In vitro* findings suggest that pathological tau may spread 'prion-like' across neuronal connections in an activity-dependent manner. Supporting this notion, functional brain networks show a spatial correspondence to tau deposition patterns. However, it remains unclear whether higher network-connectivity facilitates tau propagation. To address this, we included 55 normal aged elderly (i.e. cognitively normal, amyloid-negative), 50 Alzheimer's disease patients (i.e. amyloid-positive) covering the preclinical to dementia spectrum, as well as 36 patients with pure (i.e. amyloid-negative) vascular cognitive impairment due to small vessel disease. All subjects were assessed with AV1451 tau-PET and resting-state functional MRI. Within each group, we computed atlas-based resting-state functional MRI functional connectivity across 400 regions of interest covering the entire neocortex. Using the same atlas, we also assessed within each group the covariance of tau-PET levels among the 400 regions of interest. We found that higher resting-state functional MRI assessed functional connectivity between any given region of interest pair was associated with higher covariance in tau-PET binding in corresponding regions of interest. This result was consistently found in normal ageing, Alzheimer's disease and vascular cognitive impairment. In particular, inferior temporal tau-hotspots, as defined by highest tau-PET uptake, showed high predictive value of tau-PET levels in functionally closely connected regions of interest. These associations between functional connectivity and tau-PET uptake were detected regardless of presence of dementia symptoms (mild cognitive impairment or dementia), amyloid deposition (as assessed by amyloid-PET) or small vessel disease. Our findings suggest that higher functional connectivity between brain regions is associated with shared tau-levels, supporting the view of prion-like tau spreading facilitated by neural activity.

1 Institute for Stroke and Dementia Research, Klinikum der Universität München, Ludwig-Maximilians-Universität LMU, Feodor-Lynen Straße 17, 81377 Munich, Germany
2 Department of Neurology, Samsung Medical Center, Sungkyunkwan University School of Medicine, Seoul, Korea
3 Department of Neurology, Kangwon National University Hospital, Kangwon National University College of Medicine, Chuncheon, Republic of Korea
4 Neuroscience Center, Samsung Medical Center, Seoul, Korea

Received July 16, 2018. Revised November 27, 2018. Accepted December 21, 2018. Advance Access publication February 15, 2019

5 Department of Health Sciences and Technology, Samsung Advanced Institute of Health Sciences and Technology, Sungkyunkwan University, Seoul, Korea
6 Department of Neurology, Gangnam Severance Hospital, Yonsei University College of Medicine, Seoul, Korea
7 Department of Clinical Research Design and Evaluation, Samsung Advanced Institute of Health Sciences and Technology, Sungkyunkwan University, Seoul, Korea
8 Center for Imaging of Neurodegenerative Diseases, University of California, San Francisco

Correspondence to: Michael Ewers, PhD
Institute for Stroke and Dementia Research, Klinikum der Universität München, Ludwig-Maximilians-Universität LMU, Feodor-Lynen Straße 17, 81377 Munich, Germany
E-mail: Michael.Ewers@med.uni-muenchen.de

Keywords: functional connectivity; resting-state functional MRI; tau-PET; Alzheimer's disease; tau-spreading

Abbreviations: CN-Aβ− = cognitively normal amyloid-β-negative; ROI = region of interest; SUVR = standardized uptake value ratio; SVD = small vessel disease; VCI = vascular cognitive impairment

Introduction

In Alzheimer's disease, the emergence of amyloid plaques is followed by the formation of tau-containing neurofibrillary tangles that are closely correlated with neurodegeneration and dementia symptoms (Orr *et al.*, 2017). Different lines of research suggest that for tau, the spatial expansion of neurofibrillary tangles occurs in a hierarchical pattern during the course of Alzheimer's disease. Seminal brain autopsy studies established a systematic staging of tau pathology which starts to occur in the locus coeruleus and transentorhinal cortex, subsequently spreading to the hippocampus, anterior frontal and posterior parietal cortex, before showing a global distribution in the brain (Braak and Braak, 1991). Recent results from cross-sectional studies assessing AV1451 tau-PET in living humans could recapitulate distinct spatial patterns of tau distribution similar to those established by autopsy-based tau staging (Scheff *et al.*, 2006; Scholl *et al.*, 2016; Schwarz *et al.*, 2016). Since the successive spatial expansion of tau pathology is critical for the development of cognitive impairment in tauopathies such as Alzheimer's disease (Ossenkoppele *et al.*, 2016), understanding of those factors that are associated with the spatial tau distribution is of pivotal clinical importance (Bejanin *et al.*, 2017). Recent results from structural connectivity studies in humans and rodents suggest that the regional expansion of tau can be predicted by the axonal connectivity between brain regions (Iba *et al.*, 2013; Jacobs *et al.*, 2018). Results from preclinical *in vivo* and *in vitro* studies suggest that a 'prion-like' neuron-to-neuron transmission may underlie this gradual, connectivity-dependent pattern of tau distribution in the brain (Lace *et al.*, 2009; de Calignon *et al.*, 2012; Kaufman *et al.*, 2018). Injection of pathological tau within the hippocampus of tau transgenic mice triggered the spreading of filamentous tau to spatially remote yet anatomically connected brain regions, suggesting that spreading of pathological tau reflects an active transport along axonal connections rather than just passive diffusion to spatially adjacent regions (Clavaguera *et al.*, 2009). At the functional level, neural activity has been revealed to be an important modulator of tau seeding. Several *in vitro* and *in vivo* studies showed that higher neuronal activity triggered the release of filamentous tau from neurons ensuing micropinocytosis of pathological tau and aggregation in downstream neurons (Pooler *et al.*, 2013; Wu *et al.*, 2016; Evans *et al.*, 2018). Thus, regions that show shared neuronal activity exhibit a higher likelihood of similar tau levels. However, whether the level of regional neural activity synchronous between brain regions is related to the similarity of tau levels in those connected brain regions in humans is not clear (Seeley *et al.*, 2009). The major aim of the current combined resting-state functional MRI and tau-PET study was to test whether higher functional MRI-assessed intrinsic functional connectivity, i.e. synchronous activity between two given brain regions, is associated with stronger interregional similarity of tau deposition (i.e. tau covariance) as assessed by tau-PET.

Functional connectivity of neural activity can be non-invasively estimated via resting-state functional MRI assessed synchronicity in the blood oxygen level-dependent signal, i.e. a proxy of neuronal firing. Resting-state functional MRI studies have revealed that the brain is composed of large-scale functional networks that show highly correlated activity fluctuations between even distant brain regions (Smith *et al.*, 2009). Such intrinsic functional networks correspond largely to anatomical fibre tract connections between regions, providing an anatomical feasibility of network connectivity (Honey *et al.*, 2009). For the current cross-sectional analysis, we hypothesize that higher resting-state functional connectivity between brain regions is related to higher covariance of tau between the functionally connected brain regions (i.e. 'tau covariance'). Initial support for this notion comes from previous tau-PET imaging studies in subjects with Alzheimer's disease showing a spatial correspondence between regional prevalence of abnormal tau and major functional networks in the human brain (Hansson *et al.*, 2017; Hoenig *et al.*, 2018). A quantitative relationship between the level of resting-state functional connectivity and tau-PET, however, has rarely been

assessed. A recent combined functional MRI and tau-PET study showed that higher tau was associated with higher graph theoretical indices of functional connectivity assessed in Alzheimer's disease dementia ($n = 20$), but not primary progressive palsy (Cope *et al.*, 2018). These results support the view that functional connectivity is related to tau deposition, but raise the question whether such an association is specific to Alzheimer's disease dementia.

Albeit at a more restricted level compared to subjects in presumably early stages of Alzheimer's disease (i.e. preclinical Alzheimer's disease), higher age in amyloid-negative elderly subjects is also associated with an increase in AV1451 PET assessed tau deposition (Johnson *et al.*, 2016; Maass *et al.*, 2018). In normal ageing, higher levels of AV1451 PET detected pathological (filamentous) tau is found mainly in the medial and inferior temporal lobe (Johnson *et al.*, 2016; Scholl *et al.*, 2016). Furthermore, dramatically increased levels of tau deposition were recently reported amyloid-negative vascular cognitive impairment (VCI) (Kim *et al.*, 2018). In VCI, abnormal tau as assessed by AV1451 PET was observed in medial and inferior temporal regions, but also in adjacent medial parietal and medial frontal regions, similar to the tau pattern observed in Alzheimer's disease (Kim *et al.*, 2018).

Here, we addressed the pivotal question whether higher levels of resting-state functional connectivity are associated with higher spatial covariance of tau within normal ageing, a wider clinical spectrum of Alzheimer's disease subjects and VCI. To this end, we assessed the association between functional connectivity and higher spatial tau covariance in a larger sample of subjects ($n = 141$), including cognitively normal amyloid-negative elderly subjects ($n = 55$), amyloid-positive subjects ranging from cognitive normal to Alzheimer's disease dementia ($n = 50$), as well as amyloid-negative subjects with VCI due to small vessel disease (SVD, $n = 36$). Using resting-state functional MRI and AV1451 tau-PET data obtained in these subjects, we assessed in a whole-brain approach whether the pattern of tau deposition is associated with the underlying functional brain architecture.

Materials and methods

Participants

Normal ageing and Alzheimer's disease: ADNI

We included 105 participants from the Alzheimer's Disease Neuroimaging Initiative (ADNI) phase 3 (ClinicalTrials.gov ID: NCT02854033) based on availability of T_1-weighted and resting-state functional MRI, ^{18}F-AV1451 tau-PET for the assessment of tau and ^{18}F-AV45 amyloid-PET ($n = 87$) or alternatively ^{18}F-florbetaben amyloid-PET ($n = 18$) for the assessment of amyloid deposition. All measures had to be obtained at the same study visit. Using Freesurfer-derived global amyloid-PET (AV45/florbetaben) standardized uptake value ratio (SUVR) scores normalized to the whole cerebellum (provided by the ADNI-PET Core), all subjects were characterized as amyloid-β-positive (Aβ+) or -negative (Aβ−) based on established cut-points (global AV45 SUVR > 1.11 or global florbetaben-PET SUVR > 1.2; Table 1) (Landau *et al.*, 2012). For the normal-ageing group, we included 55 elderly cognitively normal [Mini Mental State Exanimation (MMSE) > 24, Clinical Dementia Rating (CDR) = 0, non-depressed] amyloid-β-negative subjects (CN-Aβ−). To cover the spectrum of Alzheimer's disease, we included 27 cognitively normal amyloid-β-positive (CN-Aβ+), 16 mild cognitively impaired (MCI) amyloid-β-positive subjects (MMSE > 24, CDR = 0.5, showing objective memory loss on the education-adjusted Wechsler Memory Scale II but preserved activities of daily living) and

Table 1 Sample characteristics

AD spectrum	CN-Aβ− ($n = 55$)	CN-AD ($n = 27$)	MCI-AD ($n = 16$)	Dementia-AD ($n = 7$)	*P*-value
Age, years	72.64 (6.69)	74.26 (4.39)	73.16 (7.44)	77.56 (10.75)	0.245
Gender, male/female	24/31	8/19	8/8	¾	0.542
Education	16.62 (2.29)	16.70 (2.67)	15.88 (3.22)	14.57 (2.51)	0.085
MMSE	29.15 (1.16)	29.41 (0.93)	25.5 (3.14)	23.43 (2.23)	<0.001
ADAS-Cog	9.61 (2.69)	8.98 (2.52)	16.05 (4.62)	20.38 (4.59)	<0.001
VCI (amyloid-β−)	**MCI ($n = 22$)**	**Dementia ($n = 14$)**			
Age	76.27 (6.81)	78.57 (5.83)			0.304
Gender, male/female	7/15	3/11			0.767
Education	7.64 (5.55)	6.46 (4.86)			0.522
MMSE	25.36 (3.72)	17.43 (4.20)			<0.001
SVLT	17.32 (5.20)	11.00 (5.87)			0.002
SVD composite score	1.55 (1.1)	1.43 (1.22)			0.768
WMH volume, ml	22.59 (6.10)	44.82 (10.10)			0.483
Number of lacunes	6.47 (7.51)	7.36 (7.18)			0.646
Number of microbleeds	13.37 (18.69)	25.96 (49.20)			0.212

Values are presented as mean (SD).
AD = Alzheimer's disease; ADAS-Cog = Alzheimer's disease assessment scale cognitive subscale; MMSE = Mini-Mental State Examination; SVLT = Seoul verbal learning test; WMH = white matter hyperintensity.

seven amyloid-β-positive patients with dementia (MMSE < 26, CDR > 0.5, fulfilment of NINCDS/ADRDA criteria for probable Alzheimer's disease) (Petersen *et al.*, 2010). Ethical approval was obtained by the ADNI investigators, all participants provided written informed consent.

Vascular cognitive impairment: Samsung Medical Center, Seoul

We included 36 amyloid-β-negative subjects with VCI due to SVD who were recruited from 2015 to 2016 at the Samsung Medical Center, Seoul, Korea (Leemans *et al.*, 2009). For inclusion in the current analysis, patients had to have available structural MRI and resting-state functional MRI, ^{18}F-AV1451 tau-PET and ^{18}F-florbetaben amyloid-PET all obtained at the same study visit. General study inclusion criteria have been described in detail previously (Kim *et al.*, 2016, 2018). In brief, all subjects had to show objective cognitive impairment as indicated by a test score below the age-adjusted 16th percentile in any cognitive domain including language, visuospatial, memory or executive function. Significant SVD was defined as white-matter hyperintensity burden of size >10 mm within the periventricular white matter and >25 mm in deep white matter. MCI was clinically diagnosed following the Petersen criteria (Petersen *et al.*, 2014), dementia was diagnosed following the National Institute on Aging research criteria for probable Alzheimer's disease (McKhann *et al.*, 2011). Based on Freesurfer-derived global florbetaben-PET SUVR scores (intensity normalized to the cerebellar grey matter) (Kim *et al.*, 2018), patients were defined as amyloid-β-negative (MCI/dementia = 22/14) based on a previously established cut-off at 1.45 (Villemagne *et al.*, 2011; Bullich *et al.*, 2017). The burden of SVD was graded on a scale ranging from 0 to 3, using a previously described scoring system based on SVD imaging markers (Kim *et al.*, 2018). That composite score of SVD burden (SVD score) was the sum of the presence of lacunes (score of 1 if more than four lacunes), microbleeds (score of 1 if more than four microbleeds) and white-matter hyperintensities (score of 1 if white-matter hyperintensity volume >40.6 ml). For a more detailed description of the SVD score refer to Kim *et al.* (2018). The study was approved by the Institutional Board of Samsung Medical Center, all participants provided written informed consent.

MRI and PET acquisition and preprocessing

In both samples, all MRI data were obtained on 3 T scanner systems. AV1451 tau-PET was assessed via intravenous bolus tracer injection. For details on image acquisition and sequence parameters please see the Supplementary material. AV1451 and resting-state functional MRI images were preprocessed and spatially normalized using the same SPM12-based (Wellcome Trust Centre for Neuroimaging, University College London) pipeline as described previously (Franzmeier *et al.*, 2017*a*, *b*, *c*, *d*, 2018). Details on preprocessing are provided in the Supplementary material. Note that all processing steps were conducted fully independent for the samples from ADNI and Samsung Medical Center, hence no data were merged during any stage of data processing or analysis.

Assessment of functional connectivity and tau covariance

Functional connectivity and tau covariance were estimated in a region of interest (ROI)-based manner, using 400 ROIs from the Schaefer functional MRI atlas (Fig. 1A), which is based on a data-driven functional MRI parcellation of the neocortex and argued to reflect a neurobiologically-meaningful brain parcellation (Schaefer *et al.*, 2018). The 400 ROIs can be grouped within seven large-scale functional networks (Fig. 1A) that are congruent with previous parcellations (Yeo *et al.*, 2011). This atlas is especially suited for our joint analysis of AV1451 tau-PET and functional MRI, since the ROIs are restricted to the neocortex excluding typical AV1451 off-target binding regions such as the hippocampus or basal ganglia (Marquie *et al.*, 2015; Schaefer *et al.*, 2018), which may have otherwise confounded our analyses. All analyses steps were conducted separately but in an equivalent manner for the ADNI and Seoul datasets. Prior to all analyses, the Schaefer functional MRI atlas was masked with sample-specific sharpened grey matter masks for both samples. Sharpening was based on a previously described protocol, where voxels with the higher probability of being CSF than being grey matter were discarded from the analysis (Jack *et al.*, 2017). Further, to address whether the distance between ROI-mediated associations between functional connectivity and tau, we computed the Euclidean distance between any ROI pair (Supplementary material).

To ensure that reported results were not driven by the nature of the 400 ROI Schaefer parcellation, we repeated all analyses using the 200 ROI variant of the Atlas (Schaefer *et al.*, 2018). The result pattern when using this 200 ROI parcellation was consistent with all results reported here.

Functional connectivity assessment

Functional connectivity was estimated for each subject based on fully preprocessed functional MRI data. Specifically, we extracted the mean functional MRI time course for each of the 400 ROIs by averaging the signal across voxels falling within an ROI per volume. Mean ROI time courses were then cross-correlated using Pearson-Moment correlation, yielding a 400 × 400 functional connectivity matrix that was subsequently Fisher z-transformed and autocorrelations were set to zero. For each group (i.e. CN-Aβ−, Alzheimer's disease and VCI), we then computed group-average functional connectivity matrices across subjects.

Tau covariance assessment

We assessed the correlation between the levels of tau-PET in a given region X and another region Y (see Fig. 1B for an analysis flow chart). The analysis pipeline was adopted in a modified way from previous studies using this approach to determine FDG-PET (i.e. metabolic covariance) or grey matter covariance (i.e. structural connectivity) across brain regions (Pagani *et al.*, 2014; Di *et al.*, 2017). First, we computed the mean tau-PET uptake within each of the 400 ROIs for each subject [Fig. 1B(i)]. Next, we vectorized the mean ROI data to subject-specific 400-element vectors [Fig. 1B(ii)]. Using these 400-element tau-PET uptake vectors, we then assessed across subjects the pairwise ROI-to-ROI Spearman correlation

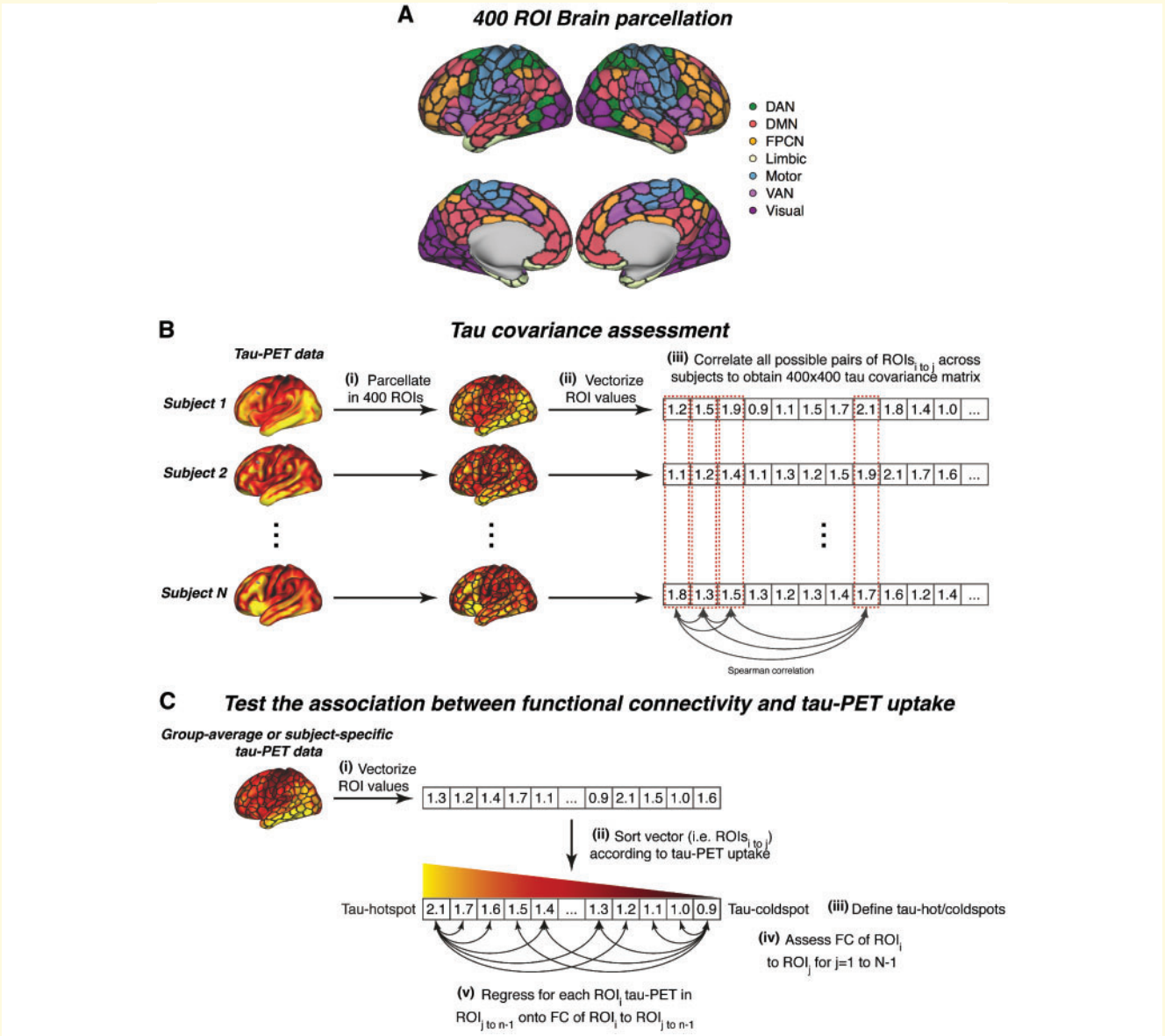

Figure 1 Analysis flow chart. (**A**) Brain parcellation scheme (Schaefer *et al.*, 2018) that was used for parcellating tau-PET and functional MRI data. (**B**) Flow chart of the tau covariance analysis. (**i**) Individual tau-PET scans are parcellated into 400 ROIs for each individual and (**ii**) mean ROI values are subsequently vectorized. Across subject tau values within a given ROI are correlated with all other ROIs using spearman-correlation (**iii**) to obtain a 400 × 400 tau covariance matrix. (**C**) Pipeline for testing the association between functional connectivity of seed ROIs and absolute tau-PET levels in target ROIs. DAN = dorsal attention network; DMN = default-mode network; FC = functional connectivity; FPCN = fronto-parietal control network; VAN = ventral attention network.

of tau-PET uptake [Fig. 1B(iii)]. We specifically used Spearman correlation to avoid that tau covariance estimation was driven by extreme tau-PET values. This analysis resulted in a single 400 × 400 sized tau covariance matrix each for each group (i.e. CN-Aβ−, Alzheimer's disease, VCI). Again, autocorrelations were set to zero and all correlations were Fisher z-transformed, equivalent to the functional connectivity matrices.

Statistics

For both samples, baseline demographics were compared between diagnostic groups within the ADNI and Seoul sample using chi-squared tests for categorical variables and ANOVAs (ADNI) or two-sample *t*-tests (Seoul) for continuous variables.

To assess the spatial distribution of pathological tau (i.e. SUVR > 1.2) (Mishra *et al.*, 2017), we averaged voxel-wise tau-PET maps within each diagnostic group. We extracted the average tau-PET uptake in a network-specific way, to assess whether tau-accumulation is constrained to certain networks.

To test our first hypothesis, i.e. that the functional connectivity between two given brain regions is associated with tau covariance between those regions, we computed spatial linear regression with the average functional connectivity matrix as

the independent variable and the tau covariance matrix as the dependent variable. This analysis was conducted separately for CN-Aβ−, Alzheimer's disease and VCI groups. Significance was assessed by repeating this linear regression on 1000 bootstrapped samples (based on which group-average functional connectivity and tau covariance matrices were iteratively determined) and applying a one-sample *t*-test on the resulting β-value distribution. We next tested whether associations between functional connectivity and tau covariance were driven by spatial proximity between ROIs, since tau is known to propagate across spatially adjacent regions (Cho *et al.*, 2016). To this end, we repeated the above described analysis this time controlling for Euclidean distance between ROIs.

We also hypothesized that at high levels of tau in seed regions, higher functional connectivity should be associated with higher tau in connected target regions. However, at lower levels of tau in seed regions, higher functional connectivity should be associated with lower levels of tau in connected target regions. The rationale is that tau propagation is a function of both the level of tau in the seed region and the level of functional connectivity between the seed region and the target region. To test this hypothesis, we vectorized [Fig. 1C(i)] and rank-ordered all ROIs by group-average tau-PET uptake [Fig. 1C(ii)]. We then assessed the group-average seed-based functional connectivity for each pair of seed and target ROIs in the brain [Fig 1C(iv)]. We next regressed the tau-PET levels in the target ROIs for a given seed ROI onto the functional connectivity values between the target ROIs and the given seed ROI. We iterated this analysis for all seed ROIs, resulting a series of β-values across the different seed ROIs [Fig. 1C(v)]. To assess whether higher tau-PET in the seed ROI is associated with higher functional connectivity related tau-PET in target ROIs, we computed across seed ROIs, the Pearson-Moment correlation between the tau-PET uptake in a seed ROI and the corresponding β-value (i.e. the association between a seed ROI's functional connectivity pattern and tau-PET uptake in the target ROIs) for a given seed ROI. To assess significance of this association we repeated the entire analysis on 1000 bootstrapped samples (based on which group-average seed functional connectivity and tau-PET uptake were iteratively determined). To illustrate the association between functional connectivity and absolute tau-PET levels we plotted the association between seed functional connectivity and tau-PET uptake for regions with maximum tau (i.e. tau-hotspots) and minimum tau (i.e. tau cold spots) [Fig. 1C(iii)]. To ensure that results were not driven by ROIs with very low tau-PET signal, we repeated this analysis in a stepwise manner, retaining only ROIs with an AV1451 tau-PET SUVR > 1.0, 1.1.

In a third step, we aimed to determine whether the interindividual variability in the association between functional connectivity and tau-PET uptake was explained by elevated amyloid-β levels or SVD burden. Here, we conducted a random effects analysis, where we first ran linear regression models to determine subject-specific associations between functional connectivity of a subjects' tau hot- or cold spot (i.e. the ROIs with maximum/minimum tau-PET uptake in a given subject) and tau-PET uptake in remaining ROIs (Fig. 1C). Using a one-sample *t*-test we assessed whether the resulting distribution of standardized β-values (i.e. the weight of the subject-level associations between tau hot- or cold spot functional connectivity and tau-PET-uptake in target regions) was significantly different than zero. We then tested whether subject-level β-values were different between CN-Aβ− and Alzheimer's disease groups using an ANCOVA, including group, age, gender, education and site as predictors. In the VCI subjects, we tested whether associations between tau hot- or cold spot functional connectivity and tau uptake were associated with SVD severity that has been previously shown to relate to increased inferior temporal tau load in this sample (Kim *et al.*, 2018). To this end, we tested whether β-values were associated with SVD composite scores or white matter hyperintensity volume, microbleed count and lacune count using linear regression, controlled for age, gender and education.

All analyses described here were conducted using R statistical software. Associations (standardized β-weights and correlations) were considered significant when meeting an alpha threshold of 0.05.

Data availability

The data that support the findings of this study will be made available upon request to the corresponding author and the Alzheimer's Disease Neuroimaging Initiative (ADNI) committee. The data from ADNI cannot be shared directly by the authors due to data protection defined by the ADNI data use policy (https://ida.loni.usc.edu/collaboration/access/appLicense.jsp).

Results

Group demographics are shown in Table 1.

Spatial distribution of abnormal tau across diagnostic groups

In agreement with previous findings, we observed a hierarchical, disease stage-dependent pattern of tau-PET uptake. In normal ageing (i.e. CN-Aβ−) abnormal tau-PET uptake was primarily restricted to the inferior lateral temporal cortex (Fig. 2A). In Alzheimer's disease (i.e. Aβ+), increasing disease severity from cognitively normal to dementia was associated gradual increasing tau-PET uptake following a typical Braak-like pattern. In VCI, abnormal tau-PET uptake was restricted to inferior temporal and frontal regions in MCI, but more widespread in VCI dementia. Regional tau-PET levels within major functional networks showed a network-specific profile of tau distribution, with tau being highest within the medial temporal limbic network, followed by elevated tau levels in other cortical networks, whereas the motor network was mostly spared (Fig. 2B). Tau burden increased in each network with increasing disease severity.

Functional connectivity is associated with tau covariance

To test whether functional connectivity between any two brain regions is associated with covarying tau-PET levels,

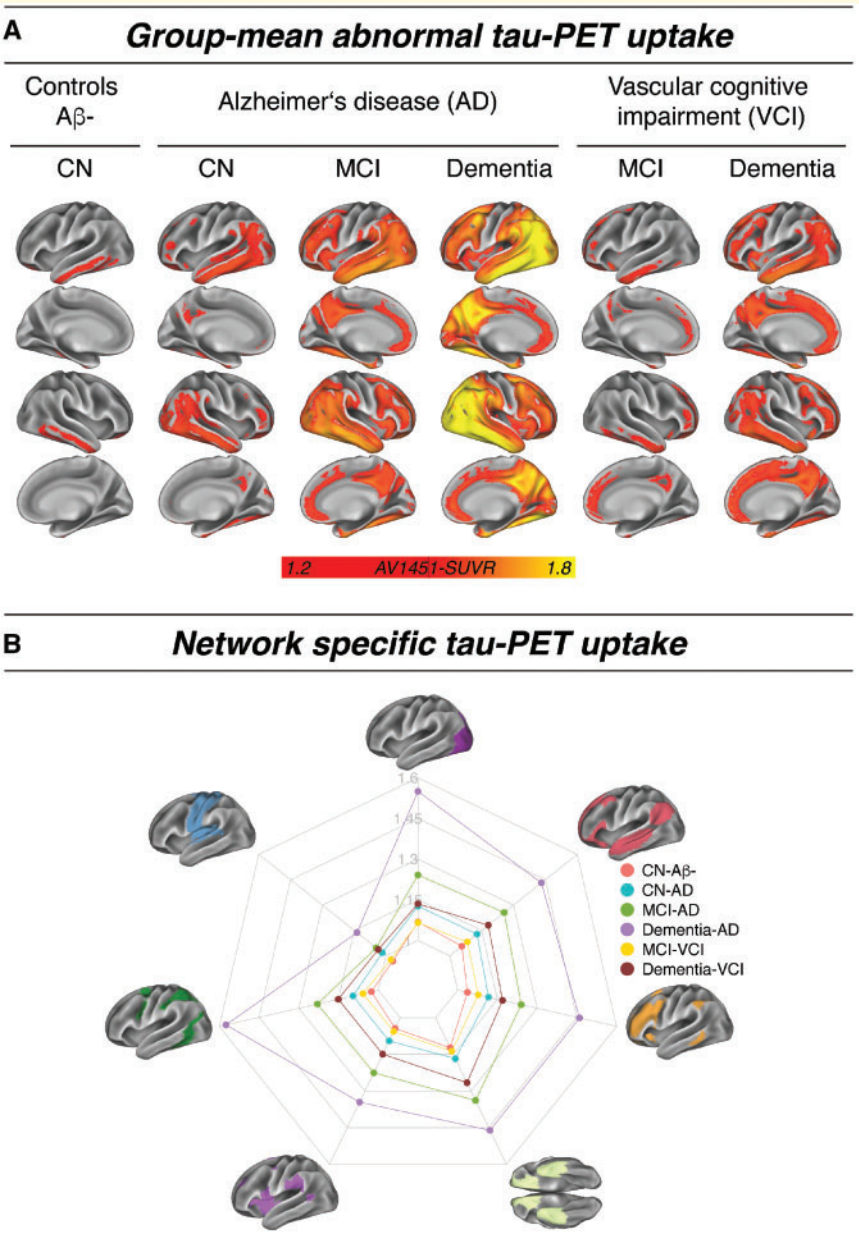

Figure 2 Group mean tau-PET data. (**A**) Mean distribution of abnormal tau (i.e. SUVR > 1.2) for each sample and diagnostic group. (**B**) Network-specific mean tau-PET SUVRs stratified by diagnostic groups. AD = Alzheimer's disease; CN = cognitively normal.

we computed the similarity between functional connectivity and tau covariance matrices (Fig. 3). Spatial regression of functional connectivity against the tau covariance matrices showed that higher functional connectivity was associated with higher tau covariance, for CN-Aβ− ($\beta = 0.299$, $P < 0.001$, Fig. 4A), Alzheimer's disease spectrum ($\beta = 0.453$, $P < 0.001$, Fig. 4B) and VCI ($\beta = 0.397$, $P < 0.001$, Fig. 4C). These results confirm our hypothesis that higher functional connectivity was associated with higher tau covariance in normal ageing, different stages of Alzheimer's disease, as well as VCI. To assess whether associations between functional connectivity and tau covariance were driven by spatial proximity between ROIs we recomputed the above described regression models, controlling for between-ROI Euclidean distance (see Supplementary material for how Euclidean distance was determined). Here, all associations between functional connectivity and tau covariance remained consistent, in the CN-Aβ− ($\beta = 0.251$, $P < 0.001$), Alzheimer's disease ($\beta = 0.354$, $P < 0.001$) and VCI sample ($\beta = 0.421$, $P < 0.001$). Mapping of tau-PET uptake within the functional network topology showed that the tau deposition clustered within closely functionally connected regions (Fig. 4D–F), suggesting that the functional topology rather than geometric distance between brain regions corresponds best to the spatial pattern of tau deposition.

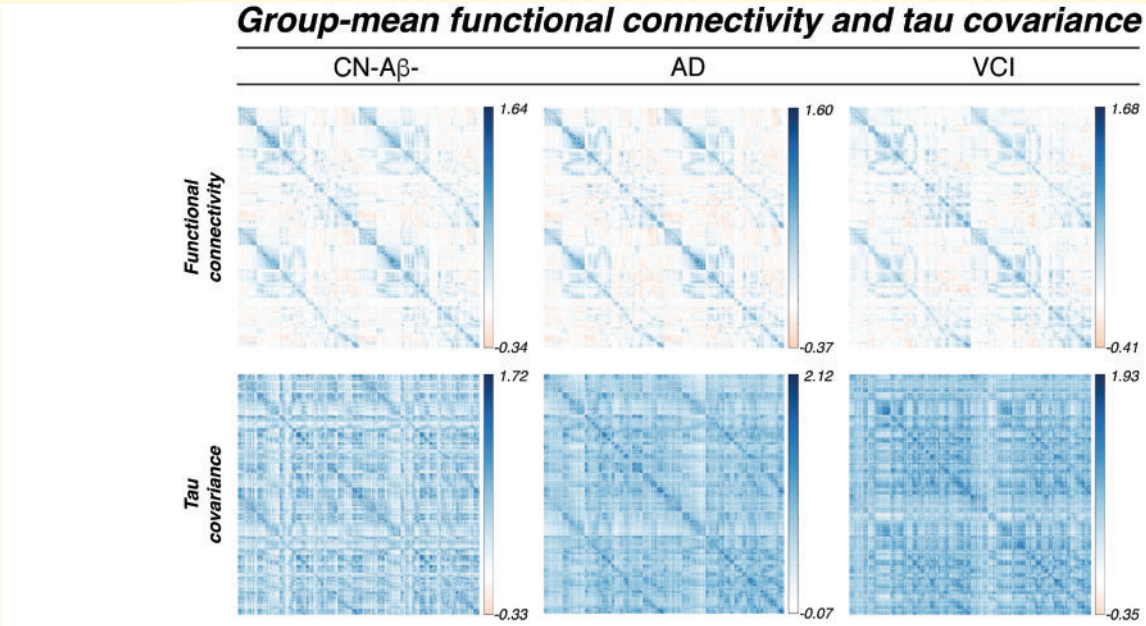

Figure 3 Group mean functional connectivity and tau covariance matrices. AD = Alzheimer's disease.

Functional connectivity predicts absolute tau-PET uptake levels

We next tested whether the level of tau-PET uptake in a given seed region is predictive of tau-PET uptake in connected target regions. For seeds with higher levels of tau, we found that higher functional connectivity was associated with higher levels of tau in target regions in all three groups including CN-Aβ−, Alzheimer's disease spectrum, and VCI. Conversely, for seeds with lower levels of tau, higher functional connectivity was associated with lower tau in target regions (Fig. 5A–C). This result pattern was reflected in a strong positive correlation between the seed ROIs tau-PET uptake and their functional connectivities' predictive weight (i.e. regression derived β-coefficient) on tau-PET uptake in target ROIs, which was consistently detected in CN-Aβ− ($\beta = 0.724$, $P < 0.001$), Alzheimer's disease spectrum (Aβ+: $\beta = 0.759$, $P < 0.001$) and VCI ($\beta = 0.611$, $P < 0.001$). Results remained consistent when restricting this entire analysis to ROIs with AV1451 tau-PET SUVRs > 1.0 or 1.1 (Supplementary Fig. 1).

To illustrate this point further, we display the results for the analysis of seed regions with peak-level of tau (tau hotspots, Fig. 5D–F) and minimum-level of tau (tau cold-spot, Fig. 5 G–I). Higher functional connectivity of the hotspot seed was associated with higher absolute levels of tau in the target regions in CN-Aβ− ($\beta = 0.469$, $P < 0.001$), Alzheimer's disease spectrum ($\beta = 0.619$, $P < 0.001$) and VCI ($\beta = 0.199$, $P < 0.001$). Conversely, higher functional connectivity of the cold spot seeds was associated with lower absolute levels of tau in target regions in CN-Aβ− ($\beta = -0.098$, $P = 0.049$), Alzheimer's disease spectrum ($\beta = -0.582$, $P < 0.001$), and VCI ($\beta = -0.293$, $P < 0.001$). This result pattern suggests that regions with high tau levels share similarly high tau levels with closely connected brain regions, while regions with low tau share similarly low tau levels with closely connected regions.

The anatomical location of tau hot or cold spots within each sample is shown in Supplementary Fig. 2.

Associations between functional connectivity and tau are not driven by amyloid-β or small vessel disease

We next asked whether the level of amyloid-β or SVD modulated the association between functional connectivity and tau covariance. To this end, we conducted subject-specific regression models, where we tested the individual association strength (i.e. β-value) between functional connectivity of a tau hot- or cold spot seed and tau-PET uptake in target regions. First, we confirmed on the subject level that higher functional connectivity of tau hotspots predicts higher tau in target regions, where we found significant positive β-weights for CN-Aβ− [mean/standard deviation (SD) = 0.23/0.16, $t(54) = 10.326$, $P < 0.001$], Alzheimer's disease spectrum [mean/SD = 0.20/0.17, $t(49) = 7.986$, $P < 0.001$] and VCI groups [mean/SD = 0.16/0.14, $t(35) = 6.722$, $P < 0.001$] as indicated by *t*-tests against zero on the β-weight distributions. Conversely, we found significant negative β-weights for tau-cold spots for CN-Aβ− [mean/SD = −0.19/0.19, $t(54) = -7.596$, $P < 0.001$], Alzheimer's disease spectrum [mean/SD = −0.22/0.16, $t(49) = -9.678$, $P < 0.001$] and VCI [mean/SD = −0.16/0.17, $t(35) = -5.596$, $P < 0.001$].

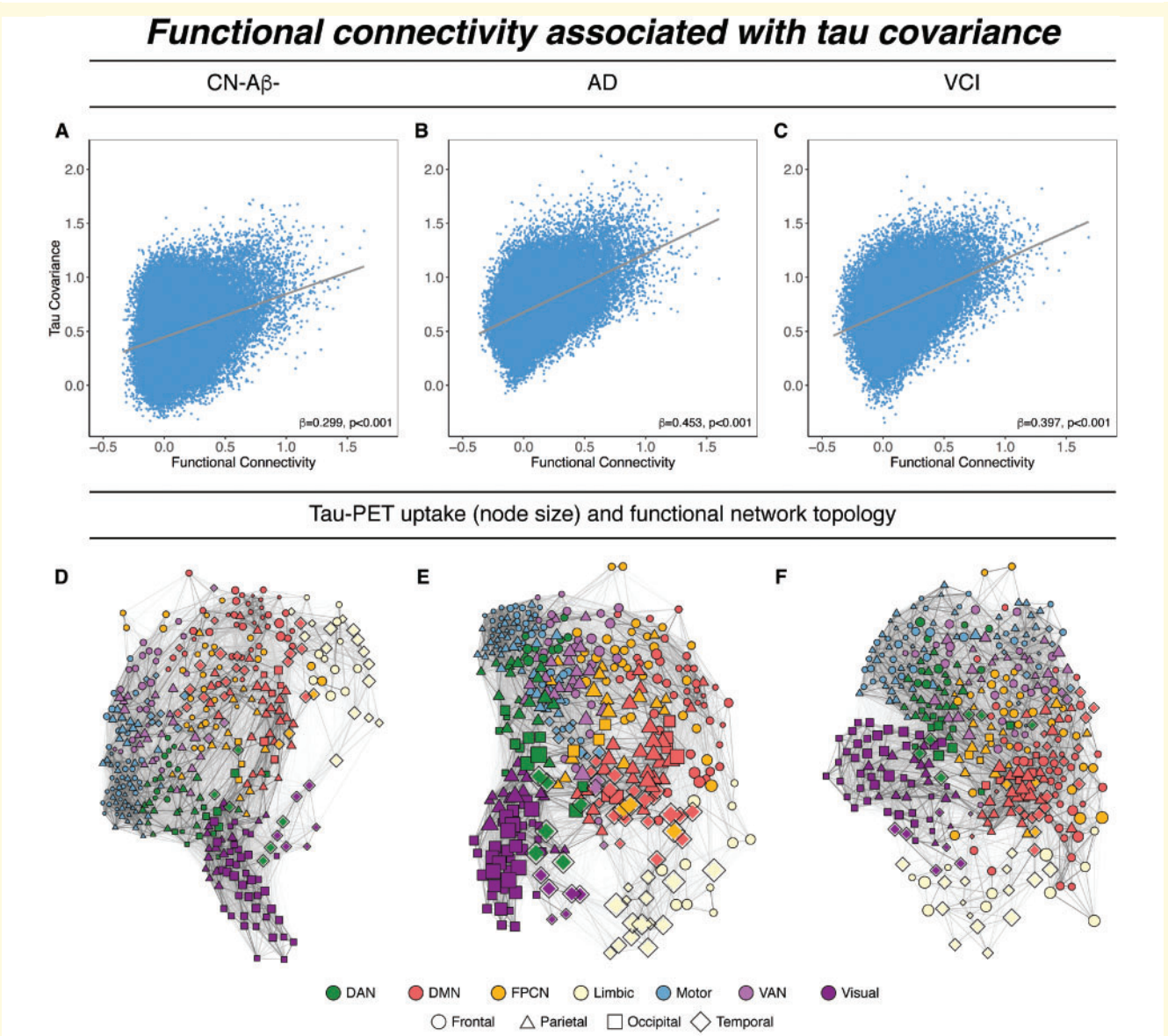

Figure 4 Associations between functional connectivity and tau covariance. Scatterplots showing the associations between tau and functional connectivity for CN-Aβ− (**A**), Alzheimer's disease (AD) (**B**), and VCI groups (**C**). Scatterplots are based on group-average data, significance for all analyses was determined using linear regression repeated on 1000 bootstrapped samples on which group-average functional connectivity and tau covariance were iteratively determined. (**D**–**F**) Force-directed graphs illustrating the association between functional network topology (node distance), tau-PET uptake (node size) and anatomical location (node symbol). Node proximity is defined based on the Fruchtermann-Reingold algorithm applied to group-average functional connectivity strength. DAN = dorsal attention network; DMN = default-mode network; FPCN = fronto-parietal control network; VAN = ventral attention network.

When testing whether abnormal amyloid-β was associated with stronger associations between functional connectivity and tau, we found no β-value differences between Alzheimer's disease spectrum and CN-Aβ− subjects for tau-hotspots [$F(5,96) = 0.941$, $P = 0.335$] or cold spots [$F(5,96) = 0.355$, $P = 0.553$; ANCOVAS controlled for age, gender, education and site].

Lastly, we assessed in the VCI sample whether SVD load influenced the association between functional connectivity and tau using linear regression adjusting for age, gender, diagnosis and education. Here, we found no association between the SVD composite scores and β-weights [hotspots: $t(30) = -0.904$, $\beta = -0.184$, $P = 0.373$; cold spots $t(30) = -0.767$, $\beta = -0.165$, $P = 0.449$]. In a similar vein, β-weights were not associated with continuous measures of white matter hyperintensity volume [hotspots: $t(30) = 0.063$, $\beta = 0.012$, $P = 0.951$; cold spots: $t(30) = -0.958$, $\beta = -0.19$, $P = 0.346$], number of micro-bleeds [hotspots: $t(30) = -0.081$, $\beta = 0.016$, $P = 0.936$; cold spots: $t(30) = -0.851$, $\beta = -0.171$, $P = 0.402$] or number of lacunes [hotspots: $t(30) = -1.371$, $\beta = 0.290$, $P = 0.181$; cold spots: $t(30) = -0.512$, $\beta = -0.117$,

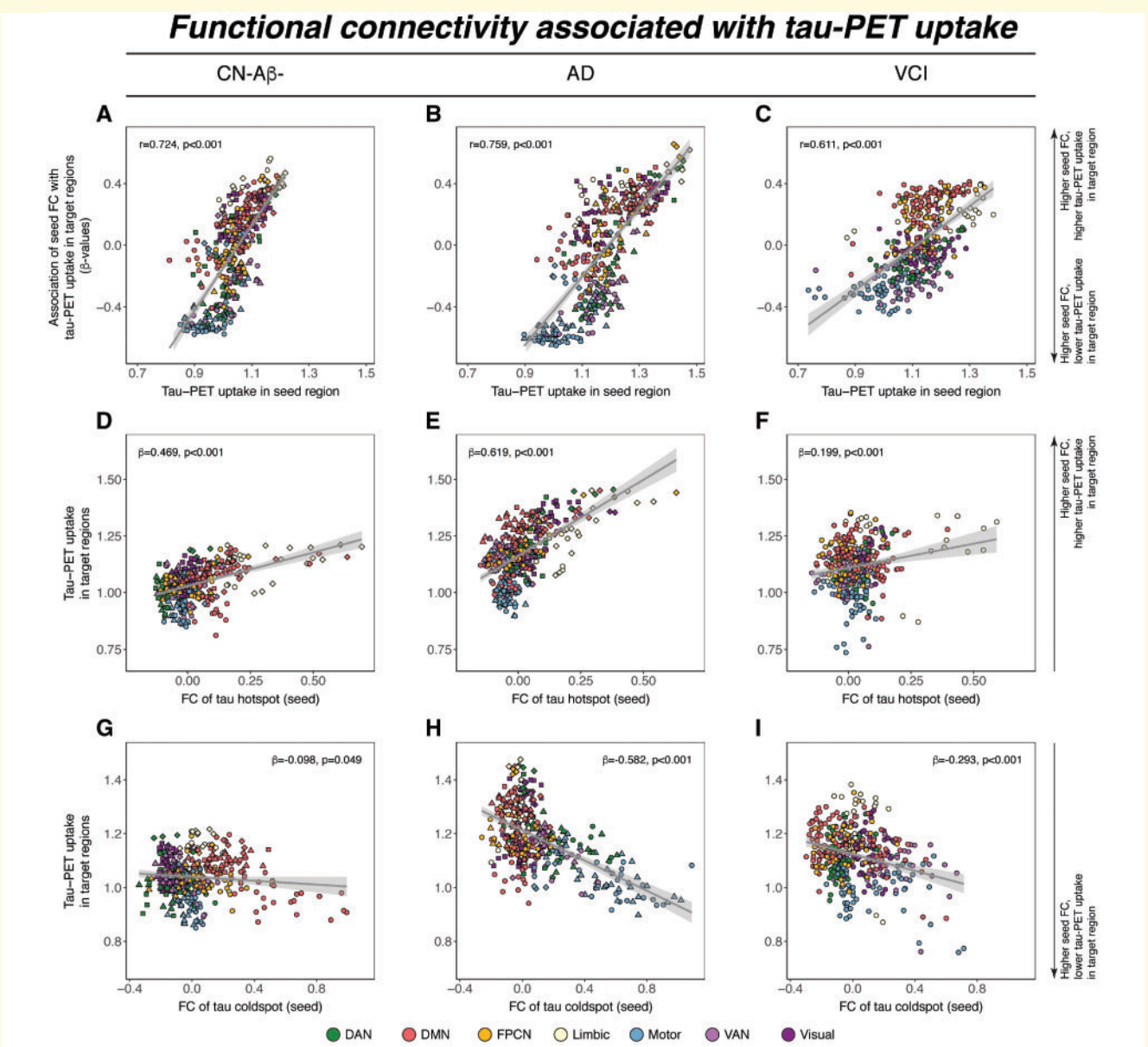

Figure 5 Functional connectivity as a predictor of tau-PET uptake. (**A**–**C**) Relationship between tau-PET uptake of a seed ROI (*x*-axis) and the regression-derived association between its' functional connectivity (FC) to target regions and tau-PET uptake in the respective target regions (*y*-axis). Positive *y*-values indicate that higher functional connectivity to target regions is associated with higher tau, while negative *y*-values indicate that higher functional connectivity to target regions is associated with lower tau. Example illustration of the results shown for regions of maximum tau (i.e. hotspots, **D**–**F**) and regions of minimum tau (i.e. cold spot, **G**–**I**). Scatterplots are based on group-average functional connectivity or tau-PET uptake, significance for all analyses was determined using linear regression repeated on 1000 bootstrapped samples on which group-average functional connectivity and group-average tau-PET uptake were iteratively determined. The anatomical location of tau hot and cold spots is shown in Supplementary Fig. 2. AD = Alzheimer's disease; DAN = dorsal attention network; DMN = default-mode network; FPCN = fronto-parietal control network; VAN = ventral attention network.

$P = 0.612$]. Results remained unchanged when using binarized measures (see 'Materials and methods' section for cut-offs) of white matter hyperintensities, lacunes or microbleeds. These results suggest that associations between functional connectivity and tau are not influenced by the presence of pathological amyloid-β levels or cerebrovascular pathology.

Discussion

The main findings of the current cross-sectional study are that (i) higher functional connectivity between any two given brain regions is associated with stronger tau covariance; (ii) for high-tau regions, higher functional connectivity predicts high tau-PET in the connected regions, but for

low-tau regions, higher functional connectivity predicts lower tau-PET in the connected regions; and (iii) all associations between functional connectivity and tau-PET were consistently detected across normal ageing (i.e. CN-Aβ−), the Alzheimer's disease spectrum and VCI. Together, these results suggest that the regional pattern of functional connectivity is predictive of the spatial pattern of tau, where the interregional tau levels covary as a function of functional connectivity, regardless of the presence of abnormal amyloid-β, cognitive impairment, or cerebrovascular pathology.

Our first finding confirms our hypothesis that levels of tau are similar (i.e. covary) between those regions that are highly functionally connected. This result is largely consistent with two recent AV1451 tau-PET studies showing that regions with covarying tau levels (i) cluster in a hierarchical manner from early- to late-Braak regions (Sepulcre *et al.*, 2017); and (ii) show a topological match with resting-state functional MRI derived functional networks in Alzheimer's disease (Hoenig *et al.*, 2018). In a similar vein, another previous study in Alzheimer's disease has shown that more widespread connectivity of a given brain region (i.e. weighted degree) was associated with higher regional tau levels, suggesting that functional hub regions are in particular susceptible to the accumulation of tau pathology (Cope *et al.*, 2018). Our results are in line with those previous reports (Cope *et al.*, 2018; Hoenig *et al.*, 2018) and point towards functional connectivity as an important factor that is predictive of regional tau-PET levels. The novelty of our current study is that the strength of functional connectivity linearly maps to the covariance of tau levels between remote brain regions, which was not only found in Alzheimer's disease but also in normal ageing and VCI. Previous *in vitro* and rodent studies have shown that optogenetically enhanced activity of tau-harbouring neurons triggered tau-release ensuing increased tau-load in postsynaptic neurons (Pooler *et al.*, 2013; Wu *et al.*, 2016). The current findings are in line with this result, showing that higher interregional functional connectivity is associated with higher covariance of tau. Although our study is correlational in nature, the results are consistent with the tau propagation model, where higher functional connectivity facilitated the seeding of tau.

Importantly, we found across all samples and groups that the strength of the association between functional connectivity and tau covariance remained almost unchanged when controlling for the Euclidian distance between regions. Thus, the link between functional connectivity and tau covariance was not driven by spatial proximity, supporting the view that tau spreads across connected regions rather than just diffusing to nearby regions (Liu *et al.*, 2012; Calafate *et al.*, 2015; Lewis and Dickson, 2016). These findings are in agreement with preclinical findings in rodents, where injection of pathological human tau (Ahmed *et al.*, 2014) or synthetically preformed tau aggregates (Iba *et al.*, 2013) caused time-dependent tau propagation to synaptically connected rather than just spatially adjacent regions.

We further showed that particular regions with peak levels of tau share high tau with functionally closely connected regions, whereas regions with very low levels of tau share low levels of tau with functionally highly connected regions. Previous studies in Alzheimer's disease could show that the functional connectivity pattern of medial temporal lobe 'atrophy hotspots' predicted similar atrophy levels in highly connected regions, an association which the authors assumed to be mediated by tau-spread from hotspots to connected regions (Mutlu *et al.*, 2017; Filippi *et al.*, 2018). The current findings support this notion, showing higher tau levels in those brain regions with high functional connectivity to tau hotspots. Given previous results of higher activity related tau spreading in transgenic mouse models of tau (Wu *et al.*, 2016), it is thus possible that higher functional connectivity of tau hotspots may facilitate the spread of tau to other brain regions. We caution, however, that our current results are cross-sectional and correlational in nature, precluding a causative interpretation. An alternative explanation of similar tau levels across functionally connected regions could be based on a regionally similar susceptibility for developing tau. Here, it has been shown previously that (i) network-forming regions exhibit similar gene expression patterns (Richiardi *et al.*, 2015); and (ii) that specific gene expression patterns can render brain regions susceptible for developing Alzheimer's disease pathology (Grothe *et al.*, 2018). Accordingly, the association between functional connectivity and tau covariance could partly be an epiphenomenon of similar function or gene expression ensuing shared susceptibility for developing tau pathology. In view of these previous findings, it is thus possible that the association between functional connectivity and tau covariance is a function of both similar local susceptibility and transneuronal propagation of tau.

We showed that the associations between functional connectivity and tau were detected not only in Alzheimer's disease but also within normal ageing (i.e. CN-Aβ−) and amyloid-β-negative subjects with VCI, suggesting that tau propagation between brain regions is associated with the level of functional connectivity, independent of amyloid-β. *In vitro* and animal studies have shown that pathological human tau propagates along connected neurons in the absence of elevated amyloid-β (Liu *et al.*, 2012; Pooler *et al.*, 2013; Calafate *et al.*, 2015; Wu *et al.*, 2016). Also, human autopsy studies have demonstrated that tau-pathology in non-demented and demented elderlies can follow a Braak-like pattern, even when amyloid-β levels are normal, which is now considered to reflect suspected non-amyloid pathology (SNAP) or primary age-related tauopathy (PART) (Crary *et al.*, 2014; Crary, 2016). Together these results suggest that tau propagation across connected regions is unlikely to be a gain of function mediated by the presence of amyloid-β. However, amyloid-β-related microglial activation (Heurtaux *et al.*, 2010) has been shown to promote local tau-hyperphosphorylation thereby increasing the

likelihood of tau spread across connected neurons (Maphis *et al.*, 2015). A recent study in Alzheimer's disease using microglia PET has indeed shown that early microglial activation can be found in inferior temporal regions, i.e. the most early occurring tau hotspots (Hamelin *et al.*, 2016). Microglia-associated tau hyperphosphorylation may cause increased local 'tau pressure' that then drives tau from hotspots to connected regions.

In the VCI sample, we found elevated tau levels in the absence of amyloid-β, consistent with previous reports in this sample (Kim *et al.*, 2018). In line with this finding, a recent post-mortem study has shown that higher systolic blood pressure—a key risk factor for VCI—is associated with higher density of tau-containing neurofibrillary tangles but not amyloid-β (Arvanitakis *et al.*, 2018). It is possible that amyloid-β-independent tau accumulation is triggered by ischaemia or chronic hypoperfusion. Rodent studies have reported that ischaemia can alter the interaction between glycogen synthase kinase 3 and protein phosphatase 2A, ensuing hyperphosphorylation of intracellular tau (Song *et al.*, 2013). However, we did not detect a modulating effect of SVD markers on the relationship between functional connectivity and tau, suggesting that this association is not moderated by SVD-related brain alterations. We caution though that the current SVD markers and composite score were primarily based on radiological global white matter alterations, and thus were not region specific. Future DTI-based fibre-tracking studies may test whether associations between functional connectivity and tau covariance are influenced specifically by the integrity of the underlying anatomical connections.

Several caveats need to be considered when interpreting the results of the current study. First, the AV1451 tau-PET tracer has been previously argued to show off-target binding in the meninges, basal ganglia, hippocampus and choroid plexus, which could potentially confound associations between functional connectivity, tau covariance and absolute tau levels (Marquie *et al.*, 2017). To address this, we *a priori* selected a brain atlas that excludes those regions typically affected by off-target binding (Schaefer *et al.*, 2018). Nevertheless, we cannot fully exclude that local increases and thus covariance in the AV1451 tau-PET signal are influenced by off-target binding.

Second, our results are exclusively based on associations between resting-state functional MRI assessed functional connectivity and tau-PET. While functional connectivity is a measure of neuronal activity shared between brain regions (Brookes *et al.*, 2011; Chang *et al.*, 2013), regions with high functional connectivity do not necessarily exhibit a direct monosynaptic structural connection (Honey *et al.*, 2009; Diaz-Parra *et al.*, 2017). Animal studies have shown that resting-state functional MRI-assessed functional connectivity can reflect multisynaptic connections (Grandjean *et al.*, 2017). Hence the currently reported associations between functional connectivity and tau covariance may reflect indirect connections along multiple intermediary connections. However, the mapping of those multi-leg connections *in vivo* is both statistically and technically difficult to date. Multivariate methods to assess complex multi-ROI connectivity patterns and advances in DTI to demonstrate smaller cortico-cortical connections, which may underlie indirect anatomical connections between grey matter regions, will enable to disentangle connections between ROIs in future studies.

Third, functional connectivity is mostly, but not entirely, matched by fibre tract connections as determined by DTI (Honey *et al.*, 2009). While the incomplete structural mappings may be partially explainable due to technical limitations of DTI (Abhinav *et al.*, 2014), it needs to be cautioned that ROI-to-ROI connections do not necessarily correspond to direct anatomical connections. Indirect cortico-cortical connections that are hard to track with current diffusion weighted imaging techniques may, however, provide the anatomical backbone for functional connectivity.

Fourth, the current study is cross-sectional in nature and thus does not assess the progression of tau pathology in the brain. To test the predictive value of functional connectivity for regional changes in tau-PET, longitudinal tau-PET studies are necessary.

Fifth, previous studies have found evidence for slightly impaired neurovascular coupling mechanisms in SVD (Lin *et al.*, 2011), which may influence functional MRI-assessed functional connectivity in the VCI group (Lawrence *et al.*, 2018). Still, we found similar patterns of the association between functional connectivity and tau covariance in patients with and without cerebrovascular disease, rendering it unlikely that the current results were influenced by altered blood oxygen level-dependent signal due to vascular changes. To overcome this limitation, future studies could employ MEG or EEG to compute functional connectivity metrics that are unbiased by impaired neuro-vascular coupling, to assess associations between functional connectivity and tau spreading in patients with SVD.

In conclusion, our results demonstrate a close correlation between functional connectivity and tau levels shared by functionally connected brain regions across normal ageing, Alzheimer's disease and VCI. These findings clearly suggest that functional connectivity plays a role in the distribution of tau and have implications for future clinical trials. Possible clinical interventions could be the silencing of overactive neural activity. A previous drug study indeed showed that suppressing hippocampal hyperactivity with levetiracetam in Alzheimer's disease improved memory (Bakker *et al.*, 2012). Future studies on drug intervention or non-invasive stimulation such as transcranial magnetic stimulation need to assess whether altering functional connectivity levels affects the progression of tau.

Acknowledgements

Part of the data used in preparation of this manuscript were obtained from the ADNI database (adni. loni.usc.edu). As such, the investigators within the ADNI study

contributed to the design and implementation of ADNI and/or provided data but did not participate in analysis or writing of this paper. A complete listing of ADNI investigators can be found online at: http://adni.loni.usc.edu/wp-content/uploads/how_to_apply/ADNI_Acknowledgement_List.pdf.

Funding

The study was funded by grants from the Alzheimer Forschung Initiative (AFI, Grant 15035 to M.E.) and European Commission (Grant 334259 to M.E.). ADNI data collection and sharing for this project was funded by the ADNI (National Institutes of Health Grant U01 AG024904) and DOD ADNI (Department of Defense award number W81XWH-12–2–0012). ADNI is funded by the National Institute on Aging, the National Institute of Biomedical Imaging, and Bioengineering, and through contributions from the following: AbbVie, Alzheimer's Association; Alzheimer's Drug Discovery Foundation; Araclon Biotech; BioClinica, Inc.; Biogen; Bristol-Myers Squibb Company; CereSpir, Inc.; Cogstate; Eisai Inc.; Elan Phar- maceuticals, Inc.; Eli Lilly and Company; EuroImmun; F. Hoffmann-La Roche Ltd and its affiliated company Genentech, Inc.; Fujirebio; GE Healthcare; IXICO Ltd.; Janssen Alzheimer Immunotherapy Research & Development, LLC.; Johnson & Johnson Phar- maceutical Research & Development LLC.; Lumosity; Lundbeck; Merck & Co., Inc.; Meso Scale Diagnostics, LLC.; NeuroRx Research; Neurotrack Technologies; Novartis Pharmaceuticals Corporation; Pfizer Inc.; Piramal Imaging; Servier; Takeda Pharma- ceutical Company; and Transition Therapeutics. The Canadian Institutes of Health Research is providing funds to support ADNI clinical sites in Canada. Private sector contributions are facilitated by the Foundation for the National Institutes of Health (www.fnih.org).

Competing interests

The authors report no competing interests.

Supplementary material

Supplementary material is available at *Brain* online.

References

Abhinav K, Yeh FC, Pathak S, Suski V, Lacomis D, Friedlander RM, et al. Advanced diffusion MRI fiber tracking in neurosurgical and neurodegenerative disorders and neuroanatomical studies: a review. Biochim Biophys Acta 2014; 1842: 2286–97.

Ahmed Z, Cooper J, Murray TK, Garn K, McNaughton E, Clarke H, et al. A novel in vivo model of tau propagation with rapid and progressive neurofibrillary tangle pathology: the pattern of spread is determined by connectivity, not proximity. Acta Neuropathol 2014; 127: 667–83.

Arvanitakis Z, Capuano AW, Lamar M, Shah RC, Barnes LL, Bennett DA, et al. Late-life blood pressure association with cerebrovascular and Alzheimer disease pathology. Neurology 2018.

Bakker A, Krauss GL, Albert MS, Speck CL, Jones LR, Stark CE, et al. Reduction of hippocampal hyperactivity improves cognition in amnestic mild cognitive impairment. Neuron 2012; 74: 467–74.

Bejanin A, Schonhaut DR, La Joie R, Kramer JH, Baker SL, Sosa N, et al. Tau pathology and neurodegeneration contribute to cognitive impairment in Alzheimer's disease. Brain 2017; 140: 3286–300.

Braak H, Braak E. Neuropathological stageing of Alzheimer-related changes. Acta Neuropathol 1991; 82: 239–59.

Brookes MJ, Woolrich M, Luckhoo H, Price D, Hale JR, Stephenson MC, et al. Investigating the electrophysiological basis of resting state networks using magnetoencephalography. Proc Natl Acad Sci USA 2011; 108: 16783–8.

Bullich S, Seibyl J, Catafau AM, Jovalekic A, Koglin N, Barthel H, et al. Optimized classification of (18)F-Florbetaben PET scans as positive and negative using an SUVR quantitative approach and comparison to visual assessment. Neuroimage Clin 2017; 15: 325–32.

Calafate S, Buist A, Miskiewicz K, Vijayan V, Daneels G, de Strooper B, et al. Synaptic contacts enhance cell-to-cell tau pathology propagation. Cell Rep 2015; 11: 1176–83.

Chang C, Liu Z, Chen MC, Liu X, Duyn JH. EEG correlates of time-varying BOLD functional connectivity. Neuroimage 2013; 72: 227–36.

Cho H, Choi JY, Hwang MS, Kim YJ, Lee HM, Lee HS, et al. In vivo cortical spreading pattern of tau and amyloid in the Alzheimer disease spectrum. Ann Neurol 2016; 80: 247–58.

Clavaguera F, Bolmont T, Crowther RA, Abramowski D, Frank S, Probst A, et al. Transmission and spreading of tauopathy in transgenic mouse brain. Nat Cell Biol 2009; 11: 909–13.

Cope TE, Rittman T, Borchert RJ, Jones PS, Vatansever D, Allinson K, et al. Tau burden and the functional connectome in Alzheimer's disease and progressive supranuclear palsy. Brain 2018; 141: 550–67.

Crary JF. Primary age-related tauopathy and the amyloid cascade hypothesis: the exception that proves the rule? J Neurol Neuromedicine 2016; 1: 53–7.

Crary JF, Trojanowski JQ, Schneider JA, Abisambra JF, Abner EL, Alafuzoff I, et al. Primary age-related tauopathy (PART): a common pathology associated with human aging. Acta Neuropathol 2014; 128: 755–66.

de Calignon A, Polydoro M, Suarez-Calvet M, William C, Adamowicz DH, Kopeikina KJ, et al. Propagation of tau pathology in a model of early Alzheimer's disease. Neuron 2012; 73: 685–97.

Di X, Gohel S, Thielcke A, Wehrl HF, Biswal BB; Alzheimer's Disease Neuroimaging Initiative. Do all roads lead to Rome? A comparison of brain networks derived from inter-subject volumetric and metabolic covariance and moment-to-moment hemodynamic correlations in old individuals. Brain Struct Funct 2017; 222: 3833–45.

Diaz-Parra A, Osborn Z, Canals S, Moratal D, Sporns O. Structural and functional, empirical and modeled connectivity in the cerebral cortex of the rat. Neuroimage 2017; 159: 170–84.

Evans LD, Wassmer T, Fraser G, Smith J, Perkinton M, Billinton A, et al. Extracellular monomeric and aggregated tau efficiently enter human neurons through overlapping but distinct pathways. Cell Rep 2018; 22: 3612–24.

Filippi M, Basaia S, Canu E, Imperiale F, Magnani G, Falautano M, et al. Changes in functional and structural brain connectome along the Alzheimer's disease continuum. Mol Psychiatry 2018. doi: 10.1038/s41380-018-0067-8.

Franzmeier N, Buerger K, Teipel S, Stern Y, Dichgans M, Ewers M, et al. Cognitive reserve moderates the association between functional network anti-correlations and memory in MCI. Neurobiol Aging 2017a; 50: 152–62.

Franzmeier N, Caballero MÁA, Taylor ANW, Simon-Vermot L, Buerger K, Ertl-Wagner B, et al. Resting-state global functional connectivity as a biomarker of cognitive reserve in mild cognitive impairment. Brain Imaging Behav 2017d; 11: 368–82.

Franzmeier N, Duering M, Weiner M, Dichgans M, Ewers M; Alzheimer's Disease Neuroimaging Initiative. Left frontal cortex connectivity underlies cognitive reserve in prodromal Alzheimer disease. Neurology 2017b; 88: 1054–61.

Franzmeier N, Duzel E, Jessen F, Buerger K, Levin J, Duering M, et al. Left frontal hub connectivity delays cognitive impairment in autosomal-dominant and sporadic Alzheimer's disease. Brain 2018; 141: 1186–200.

Franzmeier N, Gottler J, Grimmer T, Drzezga A, Araque-Caballero MA, Simon-Vermot L, et al. Resting-state connectivity of the left frontal cortex to the default mode and dorsal attention network supports reserve in mild cognitive impairment. Front Aging Neurosci 2017c; 9: 264.

Grandjean J, Zerbi V, Balsters JH, Wenderoth N, Rudin M. Structural basis of large-scale functional connectivity in the mouse. J Neurosci 2017; 37: 8092–101.

Grothe MJ, Sepulcre J, Gonzalez-Escamilla G, Jelistratova I, Scholl M, Hansson O, et al. Molecular properties underlying regional vulnerability to Alzheimer's disease pathology. Brain 2018; 141: 2755–71.

Hamelin L, Lagarde J, Dorothee G, Leroy C, Labit M, Comley RA, et al. Early and protective microglial activation in Alzheimer's disease: a prospective study using 18F-DPA-714 PET imaging. Brain 2016; 139(Pt 4): 1252–64.

Hansson O, Grothe MJ, Strandberg TO, Ohlsson T, Hagerstrom D, Jogi J, et al. Tau pathology distribution in Alzheimer's disease corresponds differentially to cognition-relevant functional brain networks. Front Neurosci 2017; 11: 167.

Heurtaux T, Michelucci A, Losciuto S, Gallotti C, Felten P, Dorban G, et al. Microglial activation depends on beta-amyloid conformation: role of the formylpeptide receptor 2. J Neurochem 2010; 114: 576–86.

Hoenig MC, Bischof GN, Seemiller J, Hammes J, Kukolja J, Onur OA, et al. Networks of tau distribution in Alzheimer's disease. Brain 2018; 141: 568–81.

Honey CJ, Sporns O, Cammoun L, Gigandet X, Thiran JP, Meuli R, et al. Predicting human resting-state functional connectivity from structural connectivity. Proc Natl Acad Sci USA 2009; 106: 2035–40.

Iba M, Guo JL, McBride JD, Zhang B, Trojanowski JQ, Lee VM. Synthetic tau fibrils mediate transmission of neurofibrillary tangles in a transgenic mouse model of Alzheimer's-like tauopathy. J Neurosci 2013; 33: 1024–37.

Jack CR Jr, Wiste HJ, Weigand SD, Therneau TM, Lowe VJ, Knopman DS, et al. Defining imaging biomarker cut points for brain aging and Alzheimer's disease. Alzheimers Dement 2017; 13: 205–16.

Jacobs HIL, Hedden T, Schultz AP, Sepulcre J, Perea RD, Amariglio RE, et al. Structural tract alterations predict downstream tau accumulation in amyloid-positive older individuals. Nat Neurosci 2018; 21: 424–31.

Johnson KA, Schultz A, Betensky RA, Becker JA, Sepulcre J, Rentz D, et al. Tau positron emission tomographic imaging in aging and early Alzheimer disease. Ann Neurol 2016; 79: 110–19.

Kaufman SK, Del Tredici K, Thomas TL, Braak H, Diamond MI. Tau seeding activity begins in the transentorhinal/entorhinal regions and anticipates phospho-tau pathology in Alzheimer's disease and PART. Acta Neuropathol 2018; 136: 57–67.

Kim H, Park S, Cho H, Jang YK, San Lee J, Jang H, et al. Assessment of extent and role of tau in subcortical vascular cognitive impairment using 18F-AV1451 positron emission tomography imaging. JAMA Neurol 2018; 75: 999–1007.

Kim HJ, Yang JJ, Kwon H, Kim C, Lee JM, Chun P, et al. Relative impact of amyloid-beta, lacunes, and downstream imaging markers on cognitive trajectories. Brain 2016; 139(Pt 9): 2516–27.

Lace G, Savva GM, Forster G, de Silva R, Brayne C, Matthews FE, et al. Hippocampal tau pathology is related to neuroanatomical connections: an ageing population-based study. Brain 2009; 132(Pt 5): 1324–34.

Landau SM, Mintun MA, Joshi AD, Koeppe RA, Petersen RC, Aisen PS, et al. Amyloid deposition, hypometabolism, and longitudinal cognitive decline. Ann Neurol 2012; 72: 578–86.

Lawrence AJ, Tozer DJ, Stamatakis EA, Markus HS. A comparison of functional and tractography based networks in cerebral small vessel disease. Neuroimage Clin 2018; 18: 425–32.

Leemans A, Jeurissen B, Sijbers J, Jones D. ExploreDTI: a graphical toolbox for processing, analyzing, and visualizing diffusion MRI data. In: Proceedings of the 17th Annual Meeting of International Society for Magnetic Resonance in Medicine, Hawaii, USA, 2009. P. 3536.

Lewis J, Dickson DW. Propagation of tau pathology: hypotheses, discoveries, and yet unresolved questions from experimental and human brain studies. Acta Neuropathol 2016; 131: 27–48.

Lin WH, Hao Q, Rosengarten B, Leung WH, Wong KS. Impaired neurovascular coupling in ischaemic stroke patients with large or small vessel disease. Eur J Neurol 2011; 18: 731–6.

Liu L, Drouet V, Wu JW, Witter MP, Small SA, Clelland C, et al. Trans-synaptic spread of tau pathology in vivo. PloS One 2012; 7: e31302.

Maass A, Lockhart SN, Harrison TM, Bell RK, Mellinger T, Swinnerton K, et al. Entorhinal tau pathology, episodic memory decline, and neurodegeneration in aging. J Neurosci 2018; 38: 530–43.

Maphis N, Xu G, Kokiko-Cochran ON, Jiang S, Cardona A, Ransohoff RM, et al. Reactive microglia drive tau pathology and contribute to the spreading of pathological tau in the brain. Brain 2015; 138(Pt 6): 1738–55.

Marquie M, Normandin MD, Vanderburg CR, Costantino IM, Bien EA, Rycyna LG, et al. Validating novel tau positron emission tomography tracer [F-18]-AV-1451 (T807) on postmortem brain tissue. Ann Neurol 2015; 78: 787–800.

Marquie M, Verwer EE, Meltzer AC, Kim SJW, Aguero C, Gonzalez J, et al. Lessons learned about [F-18]-AV-1451 off-target binding from an autopsy-confirmed Parkinson's case. Acta Neuropathol Commun 2017; 5: 75.

McKhann GM, Knopman DS, Chertkow H, Hyman BT, Jack CR Jr, Kawas CH, et al. The diagnosis of dementia due to Alzheimer's disease: recommendations from the National Institute on Aging-Alzheimer's Association workgroups on diagnostic guidelines for Alzheimer's disease. Alzheimers Dement 2011; 7: 263–9.

Mishra S, Gordon BA, Su Y, Christensen J, Friedrichsen K, Jackson K, et al. AV-1451 PET imaging of tau pathology in preclinical Alzheimer disease: defining a summary measure. Neuroimage 2017; 161: 171–8.

Mutlu J, Landeau B, Gaubert M, de La Sayette V, Desgranges B, Chetelat G. Distinct influence of specific versus global connectivity on the different Alzheimer's disease biomarkers. Brain 2017; 140: 3317–28.

Orr ME, Sullivan AC, Frost B. A brief overview of tauopathy: causes, consequences, and therapeutic strategies. Trends Pharmacol Sci 2017; 38: 637–48.

Ossenkoppele R, Schonhaut DR, Scholl M, Lockhart SN, Ayakta N, Baker SL, et al. Tau PET patterns mirror clinical and neuroanatomical variability in Alzheimer's disease. Brain 2016; 139(Pt 5): 1551–67.

Pagani M, Chio A, Valentini MC, Oberg J, Nobili F, Calvo A, et al. Functional pattern of brain FDG-PET in amyotrophic lateral sclerosis. Neurology 2014; 83: 1067–74.

Petersen RC, Aisen PS, Beckett LA, Donohue MC, Gamst AC, Harvey DJ, et al. Alzheimer's Disease Neuroimaging Initiative (ADNI): clinical characterization. Neurology 2010; 74: 201–9.

Petersen RC, Caracciolo B, Brayne C, Gauthier S, Jelic V, Fratiglioni L. Mild cognitive impairment: a concept in evolution. J Intern Med 2014; 275: 214–28.

Pooler AM, Phillips EC, Lau DH, Noble W, Hanger DP. Physiological release of endogenous tau is stimulated by neuronal activity. EMBO Rep 2013; 14: 389–94.

Richiardi J, Altmann A, Milazzo AC, Chang C, Chakravarty MM, Banaschewski T, et al. BRAIN NETWORKS. Correlated gene expression supports synchronous activity in brain networks. Science 2015; 348: 1241–4.

Schaefer A, Kong R, Gordon EM, Laumann TO, Zuo XN, Holmes AJ, et al. Local-global parcellation of the human cerebral cortex from intrinsic functional connectivity MRI. Cereb Cortex 2018; 28: 3095–114.

Scheff SW, Price DA, Schmitt FA, Mufson EJ. Hippocampal synaptic loss in early Alzheimer's disease and mild cognitive impairment. Neurobiol Aging 2006; 27: 1372–84.

Scholl M, Lockhart SN, Schonhaut DR, O'Neil JP, Janabi M, Ossenkoppele R, et al. PET imaging of tau deposition in the aging human brain. Neuron 2016; 89: 971–82.

Schwarz AJ, Yu P, Miller BB, Shcherbinin S, Dickson J, Navitsky M, et al. Regional profiles of the candidate tau PET ligand 18F-AV-1451 recapitulate key features of Braak histopathological stages. Brain 2016; 139(Pt 5): 1539–50.

Seeley WW, Crawford RK, Zhou J, Miller BL, Greicius MD. Neurodegenerative diseases target large-scale human brain networks. Neuron 2009; 62: 42–52.

Sepulcre J, Grothe MJ, Sabuncu M, Chhatwal J, Schultz AP, Hanseeuw B, et al. Hierarchical organization of tau and amyloid deposits in the cerebral cortex. JAMA Neurol 2017; 74: 813–20.

Smith SM, Fox PT, Miller KL, Glahn DC, Fox PM, Mackay CE, et al. Correspondence of the brain's functional architecture during activation and rest. Proc Natl Acad Sci USA 2009; 106: 13040–5.

Song B, Ao Q, Wang Z, Liu W, Niu Y, Shen Q, et al. Phosphorylation of tau protein over time in rats subjected to transient brain ischemia. Neural Regen Res 2013; 8: 3173–82.

Villemagne VL, Ong K, Mulligan RS, Holl G, Pejoska S, Jones G, et al. Amyloid imaging with (18)F-florbetaben in Alzheimer disease and other dementias. J Nucl Med 2011; 52: 1210–7.

Wu JW, Hussaini SA, Bastille IM, Rodriguez GA, Mrejeru A, Rilett K, et al. Neuronal activity enhances tau propagation and tau pathology in vivo. Nat Neurosci 2016; 19: 1085–92.

Yeo BT, Krienen FM, Sepulcre J, Sabuncu MR, Lashkari D, Hollinshead M, et al. The organization of the human cerebral cortex estimated by intrinsic functional connectivity. J Neurophysiol 2011; 106: 1125–65.